

https://doi.org/10.1070/QEL16920

On the feasibility of using the spiral beam formalism for analysis of cardiograms

V.G. Volostnikov, S.A. Kishkin, S.P. Kotova, M.S. Rusakova

Abstract. **A contour analysis method based on a spiral beam formalism is proposed for cardiogram classification. A cardiogram contour proximity metric is introduced in spiral beam intensity space. Normal and infarction cardiograms are classified using the proposed method. The method is shown to provide adequate results in most of the cases examined.**

Keywords: *spiral beams, classification of cardiograms, contour analysis, analysis of cardiograms.*

1. Introduction

Automated analysis of physiological signals, including electrocardiographic ones, is attracting more and more attention because there is a strong need for preventive diagnosis and early diagnosis of pathologies. Traditionally, electrocardiograms (ECGs) are analysed by a cardiology expert, who examines their shape, the height and arrangement of their waves and the position and duration of their segments [1] (Fig. 1). Analysis results depend in many respects on the doctor's skill and experience.

At the same time, more and more attention is being paid to automated analysis techniques in diagnosis. Differential diagnosis in the case of ECG analysis from the viewpoint of process automation is a classification problem, which can be solved using different approaches. One of the main methods is neural network technology [2, 3] (see also references in Isakov et al. [3]). In a number of other approaches, mathematical transformations, e.g. wavelet analysis [4, 5], are proposed as an effective tool for signal classification. However, the above-mentioned methods are not flawless: it is worth mentioning the very complex architecture of neural networks, the absence of formalised neural network adaptation algorithms and the problem of adequate neural network learning procedures. Wavelet transform algorithms typically do not take into account specific features of a signal or the purpose of signal conversion. In the case of wavelet analysis of cardiograms, there are currently no clear criteria for relating wavelet cardiograms to particular types of cardiac pathology [4]. At the same time, a cardiogram can be thought of as a particular case of a contour and, accordingly, various contour analysis methods can be used to interpret (and classify) cardiograms [6, 7].

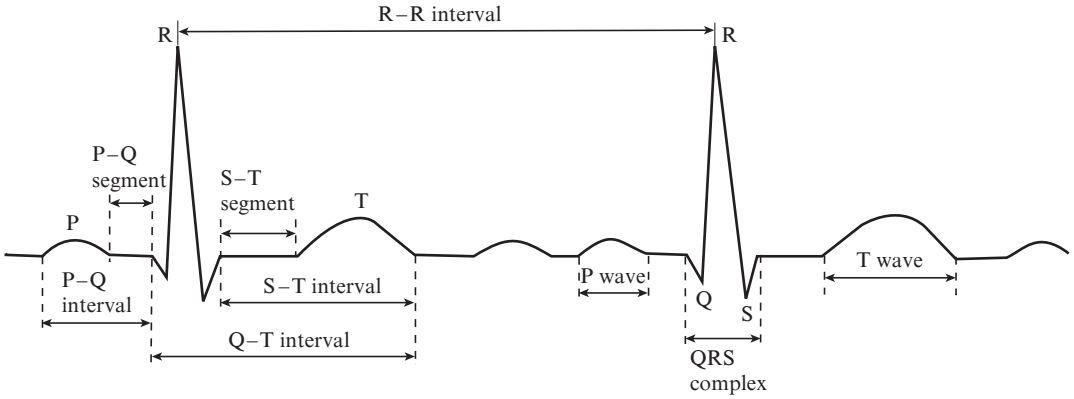

Figure 1. Schematic of a portion of a normal cardiogram (main features).

V.G. Volostnikov, S.A. Kishkin, S.P. Kotova P.N. Lebedev Physical Institute (Samara Branch), Russian Academy of Sciences, Novo-Sadovaya ul. 221, 443011 Samara, Russia;
e-mail: kotova@fian.smr.ru;
M.S. Rusakova Samara National Research University, Moskovskoe sh. 34, 443086 Samara, Russia; e-mail: r.margarita@gmail.com

Received 18 September 2018; revision received 23 November 2018
Kvantovaya Elektronika **49** (1) 83–88 (2019)
Translated by O.M. Tsarev

In previous work [8, 9], a method was proposed for contour recognition using spiral light beams. The method assumes that the object to be recognised is not a plane curve representing a contour but a corresponding spiral light beam, which is more informative and has important characteristics and properties. Spiral light beams were first considered by Abramochkin and Volostnikov [10, 11] as a class of self-similar solutions to a parabolic equation, whose intensity remains constant during evolution, to within a scale factor and rota-

tion. This work presents a continuation of previous studies [8, 9] and builds on the following background: In cardiography, contours of normal and infarction cardiograms have a characteristic shape and differ markedly from each other. Since the cardiogram waveform is described by a periodic function, one can pass from a linear time sweep to the representation of a cardiogram period as a closed contour (Fig. 2).

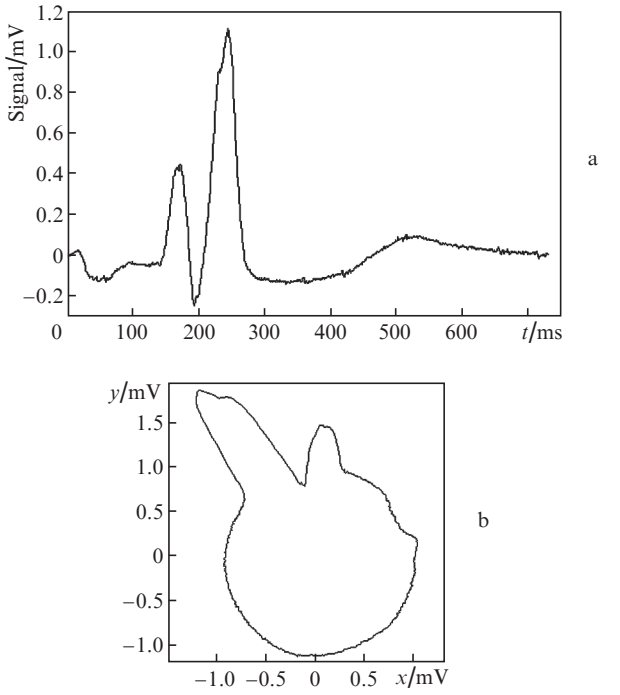

Figure 2. Portion of a cardiogram (one period) obtained from the cardiograph lead V_1 to illustrate an infarction pattern: (a) standard image in the form of a time sweep of the voltage signal $V(t)$, (b) cyclogram with $x(t) = V(t)\cos[(2\pi/T)t]$ and $y(t) = V(t)\sin[(2\pi/T)t]$.

Putting cardiogram contours in correspondence with spiral beams, one can construct some proximity (or similarity) metric for spiral beam intensity distributions (and hence for the input ECG contours) and then conclude whether a given cardiogram is normal or abnormal with an infarction pattern.

2. Mathematical formalism for spiral beam theory

In modern cardiography, use is commonly made of a standard cardiogram recording procedure, which utilises readings from 12 leads (three standard limb leads, three augmented limb leads and six chest leads), i.e. one cardiogram represents a set of data from the 12 leads. We will consider the signal from each cardiograph lead as a plane curve consisting of an ordered set of points:

$$\zeta(t) = x(t) + \mathrm{i}y(t), \quad t \in [0,T]. \tag{1}$$

Except in the case of cardiac arrhythmias, a cardiogram can be regarded as a periodic function with a period T, which allows it to be described by (1). For successful cardiogram contour analysis, it is necessary to resolve the key problems of classic contour analysis [2]: the choice of the starting point, relative scale of contours and rotation and the presence of noise. As shown earlier [8, 9], the use of the spiral beam approach for contour recognition makes it possible to obviate these problems owing to a number of inherent features of spiral light beams. A spiral beam is an optical field whose intensity distribution may have an arbitrarily complex shape (including that of a closed curve). It retains its structure during propagation and focusing to within a scale factor and rotation [11]. A contour described by (1) can be put in one-to-one correspondence with the complex amplitude of a spiral beam, $S(z,z^*)$:

$$S(z,z^*|\zeta(t),t\in[0,T]) = \exp\left(\frac{-zz^*}{\rho^2}\right) \times\int_0^T \exp\left\{-\frac{\zeta(t)\zeta^*(t)}{\rho^2}+\frac{2z\zeta^*(t)}{\rho^2} +\frac{1}{\rho^2}\int_0^t[\zeta^*(t)\,\mathrm{d}\zeta-\zeta(t)\,\mathrm{d}\zeta^*\right\}\left|\frac{\mathrm{d}\zeta}{\mathrm{d}t}\right|\mathrm{d}t, \tag{2}$$

where ρ is the Gaussian beam parameter.

If we parameterise one period of a cardiogram and represent it as a closed contour, then (if the quantisation condition for the corresponding spiral beam is met:

$$S_{\mathrm{curve}} = \frac{1}{2}\pi\rho^2 N_q, \quad N = 0,1,2\ldots, \tag{3}$$

where S_{curve} is the area under the curve and N_q is the quantisation parameter determined by the number of zeros of the complex amplitude [11]) the complex amplitude of the spiral beam is invariant to the choice of the starting point in the curve to within a phase factor [9]. Note that, for an adequate description of intricate contours, the number of zeros of the complex amplitude should not be small. In what follows, a spiral beam constructed for a large quantisation parameter ($N_q = 150$) will be referred to as a highly detailed spiral beam.

We now pass from an integral representation of complex amplitudes to infinite sums by expanding the spiral beam in terms of an orthogonal basis formed by $\mathcal{L}_{0n}(z,z^*)$ Laguerre–Gauss polynomials:

$$S(z,z^*) = \sum_{n=0}^{N} c_n\left[\sqrt{\frac{2^{n+1}}{\pi n!\rho^{2n+2}}}\exp\left(\frac{-zz^*}{\rho^2}\right)z^n\right], \tag{4}$$

where the coefficients c_n have the form

$$c_n = \sqrt{\frac{2^{n-1}\pi}{n!\rho^{2n-2}}}\int_0^T[\zeta^*(t)]^n\exp\left\{-\frac{\zeta(t)\zeta^*(t)}{\rho^2}+ +\frac{1}{\rho^2}\int_0^t[\zeta^*(\tau)\zeta'(\tau)-\zeta(\tau)\zeta'^*(\tau)\,\mathrm{d}\tau\right\}|\zeta'(t)|\mathrm{d}\tau. \tag{5}$$

As shown earlier [8, 9], if the quantisation condition (3) is met the complex amplitude of a spiral beam is sel-similar under a contour scale transformation (A) and contour rotation (α) of the form $\zeta(t) \to \zeta(t)A\times\exp(\mathrm{i}\alpha)$,

$$S(z,z^*|\zeta(t)A\exp(\mathrm{i}\alpha)) = S\left(\frac{z}{A\exp(\mathrm{i}\alpha)},\frac{z^*}{A\exp(-\mathrm{i}\alpha)}|\zeta(t)\right), \tag{6}$$

and the series expansion coefficients c_n in (4) bear information about the rotation angle.

In other words, a contour analysis problem can be solved using principles of coherent optics because the mathematical tools for describing spiral light beams allow the above-mentioned difficulties to be overcome.

3. Classification of cardiograms using the spiral beam formalism: basic principle and metric

Consider a formal problem formulation. Let a $\zeta(t)$ contour be a portion of the waveform from one of the 12 cardiograph leads over the period of the cardiac rhythm, K be the set of contours of all cardiograms from all the leads, and D be a finite set of classes of cardiograms (diagnoses). We assume that there is an unknown target dependence ($K \to D$ mapping) whose values are only known for elements of a finite learning subset $K_0 = \{(k_1, d_1), \ldots (k_n, d_m)\}$, where K_0 is a set of reference cardiograms with known diagnoses. For any cardiogram $k \in K$, it is necessary to find the corresponding class $d_j \in D$ so as to minimise the discrepancy between the set of contours k_i from the cardiograph leads and the corresponding elements of set $K_j \in K$, $K_j \to d_j$. In other words, the classification problem in this formulation can be reduced to finding an appropriate metric μ defining the distance between a contour under examination and the set of contours of the reference cardiograms from the corresponding leads. Finding such a metric is generally a nontrivial issue [12] and determines in many respects the success of a particular approach to solving the classification problem. Well-known methods of solving the classification problem (probabilistic ones, the C-means method, KNN and others) introduce frequently used metrics [12, 13] which are obviously inapplicable in the case of spiral beams because here a new metric should be invariant to contour scale transformations and rotations and also to the choice of the starting point of the contour.

We introduce the following metric μ: $I \times I \to [0, 1]$ in spiral beam intensity space, where $I(z, z^*) = S(z, z^*)S^*(z, z^*)$. As a basis, we take the intensity overlap function $\Pi(\theta)$:

$$\Pi(\theta) = \iint\limits_{\mathbb{R}^2} I^{(1)}(z, z^*) I^{(2)}(z\exp(\mathrm{i}\theta), z^*\exp(-\mathrm{i}\theta))\,\mathrm{d}x\mathrm{d}y \times \left[\sqrt{\iint\limits_{\mathbb{R}^2} I^{(1)}(z, z^*) I^{(1)}(z\exp(\mathrm{i}\theta), z^*\exp(-\mathrm{i}\theta))\,\mathrm{d}x\mathrm{d}y} \times \sqrt{\iint\limits_{\mathbb{R}^2} I^{(2)}(z, z^*) I^{(2)}(z\exp(\mathrm{i}\theta), z^*\exp(-\mathrm{i}\theta))\,\mathrm{d}x\mathrm{d}y}\right]^{-1}. \quad (7)$$

Since $\Pi(\theta)$ is a normalised scalar product, its magnitude lies within the [0, 1] segment. Let us now introduce the metric μ in the form

$$\mu(I_1, I_2) = 1 - \max_{\theta \in [0, 2\pi]} |\Pi(I_1, I_2, \theta)|. \quad (8)$$

A value of the metric as close to zero as possible means that the cardiogram under test falls in the class of cardiograms in question (there is a coincidence with a classified contour), whereas a value near unity suggests that the contour does not belong to the class under consideration.

4. Algorithm of cardiogram classification by the spiral beam method

Consider in greater detail the cardiogram classification procedure. Data for cardiogram interpretation were borrowed from the open-access physiologic signal database physionet.org [14] (PTB Diagnostic ECG Database [15]). For definiteness, we will consider two large classes of cardiograms: normal ones and cardiograms of myocardial infarction patients. Various infarction locations are possible: anterior, inferior, lateral, ventricular, septal or atrial infarction [1]. The characteristic pattern of changes in the signals from the different cardiograph leads depends on infarction location. In particular, anterior infarction is suggested by changes in leads I (II), aVL, V_1 and V_2 (V_3–V_6); inferior infarction, by changes in leads II, III and aVF; and lateral infarction, by changes in leads I, II, aVL, V_5 and V_6 [1]. Accordingly, correlations between a cardiogram under test and a reference in some leads may point to infarction.

The cardiogram comparison procedure involves the following steps:

1. The heartbeat period is determined for each cardiogram under test (to be classified), and a parameterised closed curve (1) is constructed (one period) for each of the 12 standard leads.

2. The coefficients of expansion (5) for the complex amplitude of the spiral beam (4) are calculated for each of the 12 input contours of the ECG under test. It is necessary that the quantisation condition (3) be met, where the quantisation parameter (and hence the number of series expansion coefficients) should not be small, because the contour has a rather complex shape, which requires a detailed analysis.

3. For each reference cardiogram and each of the 12 leads, precalculated series expansion coefficients are retrieved from file storage.

4. Metric (8) is calculated using all the reference cardiograms for each of the 12 leads of the cardiogram under test, and the best result is selected for each lead.

5. The results for the 12 leads are analysed and a decision is made as to how to classify the cardiogram according to the following rules:

(a) the cardiogram is classified with certainty as normal if the metric reaches a minimum in the class of normal ECGs for at least eight leads and the rest of the leads are not determining for the classes of infarction ECGs; and

(b) the cardiogram is classified with certainty as indicative of infarction if the metric reaches a minimum in the class of infarction ECGs for at least half of the leads and, moreover, these leads are determining for the infarction locations of the corresponding reference cardiograms.

5. Cardiogram classification results

As reference cardiograms, we used ten normal cardiograms of ten patients of different ages and sex and ten infarction cardiograms of ten different patients with different infarction locations (anterior, inferior, inferolateral, inferoposterolateral, anteroseptal and recurrent anterior infarctions). For each cardiogram, we constructed a closed contour over one period for the 12 leads and calculated the coefficients in the expansion of the spiral beam in terms of Laguerre–Gauss polynomials for all the contours. Next, for each cardiogram under test and each of the 12 leads, we calculated the correla-

tion function (7) with all the reference ECGs in the cases of a medium detail level (50 zeros of the complex amplitude and 300 series expansion coefficients) and a high detail level (150 zeros of the complex amplitude and 600 series expansion coefficients). Note that, even in the case of the medium detail level, we obtained good cardiogram contour recognition and classification results, but in what follows we will consider and discuss the results obtained at the high detail level. In Table 1 and below, the following designations are used: TI_k, infarction cardiograms under test; TN_k, normal cardiograms under test; EI_k, infarction reference cardiograms; and EN_k, normal reference cardiograms (the designations in round brackets are taken from an input signal database).

Table 1. Number of leads for which the best metric was reached between the cardiogram under test and normal ($\aleph_{norm}$) or infarction ($\aleph_{hat}$) reference cardiograms.

Cardiogram under test	$\aleph_{hat}$	$\aleph_{norm}$	Classification result	Actual diagnosis
TI_1 (pat_5b)	5	7	Normal ECG, controversial result	Infarction
TI_2 (pat_6b)	10	2	Infarction	Infarction
TI_3 (pat_7c)	11	1	Infarction	Infarction
TI_4 (pat_9)	9	3	Infarction	Infarction
TI_5 (pat_10a)	6	6	Infarction	Infarction
TI_6 (pat_14b)	8	4	Infarction	Infarction
TI_7 (pat_15a)	6	6	Infarction	Infarction
TI_8 (pat_16a)	6	6	Infarction	Infarction
TI_9 (pat_17b)	4	8	Normal ECG, controversial result	Infarction
TI_{10} (pat_19c)	6	6	Infarction	Infarction
TI_{11} (pat_20c)	11	1	Infarction	Infarction
TN_1 (pat_105)	4	8	Normal ECG, controversial result	Normal ECG
TN_2 (pat_245)	4	8	Normal ECG, controversial result	Normal ECG
TN_3 (pat_252)	1	11	Normal ECG	Normal ECG
TN_4 (pat_266)	1	11	Normal ECG	Normal ECG
TN_5 (pat_267)	2	10	Normal ECG	Normal ECG
TN_6 (pat_277)	4	8	Normal ECG	Normal ECG
TN_7 (pat_279a)	2	10	Normal ECG	Normal ECG
TN_8 (pat_284)	1	11	Normal ECG	Normal ECG

We tested 11 infarction cardiograms, of which 9 were classified as indicative of infarction, and 8 normal cardiograms, of which 6 were identified with certainty (classified as normal). Thus, according to the present results, the selectivity of the method is 82% and its specificity is 75%.

Consider, for example, the TI_2 cardiogram. It corresponds to a complex recurrent infarction pattern, which should be analysed with attention paid to leads I, aVL (Fig. 3), V_1, V_2, II, III and aVF. It is clearly seen in Fig. 3 that, for the infarction pattern under consideration, the cardiogram contours in lead aVL have characteristic features and differ markedly from each other even when compared visually. Objects used in the method under consideration – spiral beams – 'inherit' the initial signal geometry. Accordingly, the spiral beams differ in intensity and field phase distributions.

Tables 2 and 3 present calculated proximity metrics (μ) of the cardiogram under test with all the references.

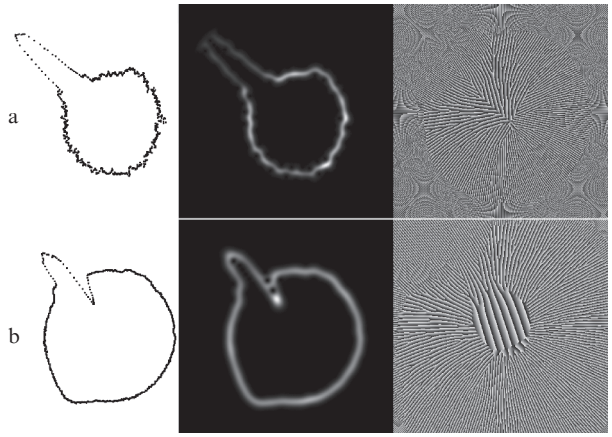

Figure 3. Contours of (a) the TI_2 infarction cardiogram under test and (b) the EN_1 normal reference cardiogram from lead aVL (left panels), intensity distributions of the corresponding spiral beams (middle panels) and phase distributions of the spiral beams (right panels). In the phase distributions, black and white pixels correspond to 0 and 2π, respectively.

Table 2. Proximity metric μ for leads I, II, III, aVL, aVR and aVF of the TI_2 cardiogram (pathology, infarction) with the corresponding leads of reference cardiograms.

Reference cardiogram	Cardiograph lead					
	I	II	III	aVL	aVR	aVF
EN_1 (pat_104)	0.625	0.693	0.776	0.591	0.267	0.758
EN_2 (pat_242)	0.588	0.644	0.796	0.617	0.577	0.756
EN_3 (pat_244)	0.479	0.604	0.726	0.497	0.367	0.670
EN_4 (pat_246)	0.432	0.589	0.735	0.523	0.317	0.725
EN_5 (pat_247)	0.368	0.702	0.756	0.574	**0.165**	0.733
EN_6 (pat_248)	0.639	0.725	0.635	0.502	0.328	0.771
EN_7 (pat_251)	0.367	0.550	0.364	0.366	0.336	0.453
EN_8 (pat_255)	0.456	0.675	0.760	0.549	0.355	0.763
EN_9 (pat_260)	0.477	0.721	0.816	0.616	0.429	0.779
EN_{10} (pat_264)	0.451	0.590	0.677	0.572	0.453	0.669
EI_1 (pat_1)	0.423	0.612	0.452	0.383	0.660	0.495
EI_2 (pat_2)	0.604	0.633	0.627	0.621	0.485	0.558
EI_3 (pat_3)	0.556	0.639	0.397	0.637	0.269	0.482
EI_4 (pat_4a)	0.367	0.621	0.231	0.486	0.311	0.445
EI_5 (pat_7a)	0.515	0.596	0.257	0.468	0.460	0.436
EI_6 (pat_8a)	0.405	0.569	0.599	0.450	0.326	0.597
EI_7 (pat_11a)	**0.350**	**0.535**	0.347	**0.333**	0.182	**0.318**
EI_8 (pat_12a)	0.542	0.578	0.215	0.452	0.321	0.522
EI_9 (pat_13a)	0.565	0.617	**0.214**	0.484	0.373	0.387
EI_{10} (pat_18a)	0.520	0.622	0.237	0.474	0.568	0.399

Note: The best metric values and the corresponding cardiograms are indicated by bold type.

Let us analyse the data obtained here. There are only two coincidences with normal ECGs, in leads aVR and V_6, whose signals are, generally speaking, not determining in diagnosing this infarction pattern. It can be stated with certainty that there is good agreement with the infarction cardiograms in leads II, aVF and V_1–V_5 (which are determining for the reference cardiograms under consideration), where the metric has minimum values (0.060–0.132). The highest value of μ in this example is 0.535 (but it is the best value in the entire set of references in lead II). There are also coincidences with the infarction cardiograms in the nondetermining leads I, III and

Table 3. Proximity metric μ for leads V_1–V_6 of the TI_2 cardiogram (pathology, infarction) with the corresponding leads of reference cardiograms.

Reference cardiogram	Cardiograph lead					
	V_1	V_2	V_3	V_4	V_5	V_6
EN_1	0.218	0.293	0.460	0.741	0.776	0.719
EN_2	0.586	0.316	0.359	0.384	0.325	0.547
EN_3	0.449	0.652	0.755	0.755	0.673	0.360
EN_4	0.267	0.285	0.371	0.468	0.409	0.399
EN_5	0.147	0.148	0.266	0.424	0.428	0.502
EN_6	0.387	0.652	0.813	0.807	0.790	0.617
EN_7	0.284	0.253	0.319	0.483	0.671	**0.344**
EN_8	0.231	0.327	0.398	0.545	0.564	0.383
EN_9	0.380	0.351	0.386	0.449	0.559	0.480
EN_{10}	0.412	0.456	0.501	0.745	0.763	0.470
EI_1	0.769	0.750	0.729	0.590	0.449	0.587
EI_2	0.512	0.431	0.280	0.247	0.396	0.477
EI_3	0.380	0.432	0.602	0.798	0.694	0.416
EI_4	**0.060**	**0.118**	**0.132**	**0.231**	0.310	0.407
EI_5	0.164	0.167	0.168	0.255	0.409	0.399
EI_6	0.587	0.664	0.724	0.812	0.808	0.423
EI_7	0.289	0.206	0.353	0.594	0.572	0.399
EI_8	0.248	0.283	0.319	0.343	0.313	0.422
EI_9	0.170	0.193	0.270	0.451	0.485	0.429
EI_{10}	0.640	0.412	0.331	0.386	**0.292**	0.528

Note: The best metric values and the corresponding cardiograms are indicated by bold type.

aVL, which also suggests that the ECG under test can be classified as indicative of infarction.

Tables 4 and 5 present calculated proximity metrics (μ) of the normal cardiogram under test with all the references. It is seen that, in 11 leads, the metric μ for the TN_3 cardiogram with the normal reference cardiograms (without pathology) has a minimum in the range 0.048–0.334, and only in lead V_5 there is a correlation with the EI_6 infarction ECG. On the other hand, since in the case of the EI_6 cardiogram characteristic changes are seen in leads II, III and aVF, without showing up in lead V_5, it is reasonable to conclude that the TN_3 cardiogram under test was successfully identified as normal (without pathology).

Table 4. Proximity metric μ for leads I, II, III, aVL, aVR and aVF of the TN_3 cardiogram (normal) with the corresponding leads of reference cardiograms.

Reference cardiogram	Cardiograph lead					
	I	II	III	aVL	aVR	aVF
EN_1	0.315	0.318	0.660	0.745	0.126	0.450
EN_2	0.729	**0.247**	0.657	0.771	0.199	0.371
EN_3	0.425	0.341	0.496	0.601	0.065	0.405
EN_4	0.542	0.422	0.612	0.465	0.242	0.432
EN_5	0.609	0.504	0.733	0.794	0.259	0.559
EN_6	0.456	0.506	**0.275**	0.376	0.110	0.317
EN_7	**0.246**	0.580	0.390	**0.334**	0.101	0.693
EN_8	0.477	0.314	0.668	0.684	0.117	0.337
EN_9	0.505	0.289	0.763	0.770	**0.048**	0.544
EN_{10}	0.452	0.297	0.328	0.724	0.077	**0.282**
EI_1	0.682	0.650	0.683	0.669	0.534	0.670
EI_2	0.724	0.656	0.645	0.685	0.356	0.662
EI_3	0.601	0.706	0.643	0.704	0.286	0.739
EI_4	0.637	0.683	0.564	0.755	0.278	0.727
EI_5	0.416	0.751	0.568	0.465	0.207	0.768
EI_6	0.388	0.465	0.400	0.699	0.148	0.590
EI_7	0.554	0.690	0.484	0.629	0.267	0.683
EI_8	0.440	0.773	0.613	0.477	0.205	0.764
EI_9	0.384	0.544	0.572	0.452	0.219	0.734
EI_{10}	0.464	0.731	0.504	0.411	0.419	0.755

Note: The best metric values and the corresponding cardiograms are indicated by bold type.

Table 5. Proximity metric μ for leads V_1–V_6 of the TN_3 cardiogram (normal) with the corresponding leads of reference cardiograms.

Reference cardiogram	Cardiograph lead					
	V_1	V_2	V_3	V_4	V_5	V_6
EN_1	0.128	0.172	0.440	0.379	0.248	0.435
EN_2	0.346	0.263	0.468	0.713	0.777	0.733
EN_3	0.125	0.530	0.641	**0.176**	0.517	0.427
EN_4	0.205	0.363	0.550	0.670	0.667	0.478
EN_5	0.160	0.346	0.592	0.682	0.653	0.327
EN_6	0.088	0.547	0.716	0.518	0.184	**0.155**
EN_7	0.087	0.147	0.436	0.694	0.495	0.300
EN_8	0.113	0.151	0.430	0.628	0.613	0.237
EN_9	0.097	**0.084**	0.352	0.703	0.649	0.222
EN_{10}	**0.063**	0.140	**0.190**	0.292	0.225	0.228
EI_1	0.768	0.736	0.639	0.621	0.800	0.705
EI_2	0.384	0.504	0.507	0.771	0.789	0.772
EI_3	0.500	0.362	0.361	0.210	0.382	0.695
EI_4	0.404	0.369	0.479	0.770	0.738	0.618
EI_5	0.167	0.283	0.492	0.777	0.799	0.722
EI_6	0.425	0.492	0.529	0.234	**0.133**	0.288
EI_7	0.113	0.311	0.531	0.646	0.611	0.424
EI_8	0.245	0.390	0.577	0.705	0.773	0.727
EI_9	0.158	0.283	0.497	0.671	0.635	0.308
EI_{10}	0.441	0.316	0.445	0.717	0.770	0.747

Note: The best metric values and the corresponding cardiograms are indicated by bold type.

Figure 4 shows spiral beam intensity distributions for the EI_9 (infarction) and EN_3 (normal) reference cardiograms in the 12 leads. It is seen that the intensity distributions in different leads have characteristic features for the infarction and normal (pathology-free) cardiograms and differ markedly. The contour proximity metric calculated by the proposed method is $\mu > 0.5$ for 8 of the 12 leads, and only in leads V_1, V_6 and aVR is μ below 0.35 (the contours obtained in these leads are sufficiently similar). It is seen from this example of proximity metric calculation for two reference cardiograms of different classes that a decision as to the classification result should rely on analysis of the metrics obtained in all the cardiograph leads. This procedure lies in the field of the theory of decision making under conditions of uncertainty and is beyond the scope of this work, but it will receive considerable attention in our future work, which we plan to focus on statistical analysis of a set of reference cardiograms and subsequent retrieval of information about similarity in terms of the proposed metric.

6. Conclusions

A spiral beam formalism has been proposed for electrocardiogram classification, a proximity metric has been introduced for the spiral beam intensity distribution, and results of

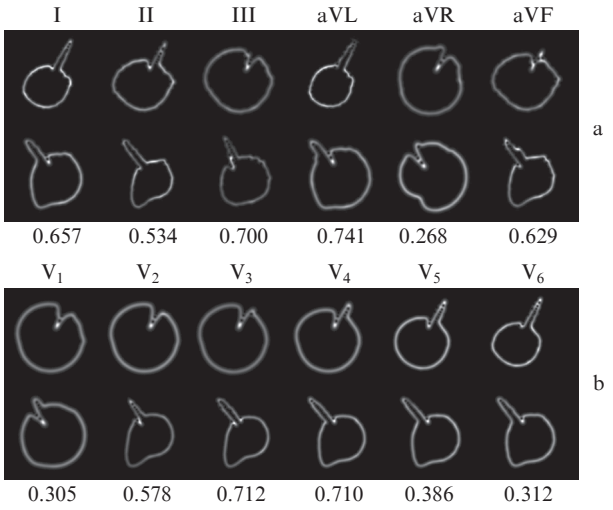

Figure 4. Spiral beam intensity distributions and contour proximity metrics (μ) in leads (a) I, II, III, aVL, aVR, aVF and (b) V_1-V_6 for the EI_9 infarction ECG (upper row) and EN_3 normal ECG (lower row).

cardiogram classification by the proposed method have been presented. The results demonstrate a successful classification for most of the cardiograms considered. The method allows one to gain information about potential infarction. As a continuation of this research, future work is expected to extend the basis for differential diagnosis of other cardiovascular pathologies, as well as for differential diagnosis of infarction location. Another applied research direction will be concerned with computation acceleration, e.g. by parallelising the algorithms involved.

Acknowledgements. This work was supported by the Russian Foundation for Basic Research (Grant No. 17-42-630934).

References

1. Orlov V.N. *Rukovodstvo po elektrokardiografii* (Manual of Electrocardiography) (Moscow: Meditsinskoe Informatsionnoe Agenstvo, 2017).
2. Haykin S. *Neural Networks: A Comprehensive Foundation* (New Jersey: Pearson Education, 2009).
3. Isakov R.V., Al Mabruk M.A., Sushkova L.T. *Med. Tekh.*, **3**, 18 (2011).
4. Romanets I.A., Atopkov V.A., Guriya G.T. *Komp'yut. Issled. Modelirovanie*, **4**, 895 (2012).
5. Krasovitskaya K.A., Cherkashin E.A. *Obrazovat. Resursy Tekhnol.*, **2**, 180 (2016).
6. Furman Ya.A. *Vvedenie v konturnyi analiz i ego prilozheniya k obrabotke izobrazhenii i signalov* (Introduction to Contour Analysis and Its Applications in Image and Signal Processing) (Moscow: Fizmatlit, 2003).
7. Dyudin M.V., Povalyaev A.D., Podval'nyi E.S., Tomakova R.A. *Vestn. Voronezhsk. Gos. Tekh. Univ.*, **10**, 54 (2014).
8. Volostnikov V.G., Kishkin S.A., Kotova S.P. *Quantum Electron.*, **43**, 646 (2013) [*Kvantovaya Elektron.*, **43**, 646 (2013)].
9. Volostnikov V.G., Kishkin S.A., Kotova S.P. *Quantum Electron.*, **48**, 268 (2018) [*Kvantovaya Elektron.*, **48**, 268 (2018)].
10. Abramochkin E.G., Volostnikov V.G. *Phys. Usp.*, **47**, 1177 (2004) [*Usp. Fiz. Nauk*, **174**, 1273 (2004)].
11. Abramochkin E.G., Volostnikov V.G. *Sovremennaya teoriya gaussovykh puchkov* (Modern Theory of Gaussian Beams) (Moscow: Fizmatlit, 2010).
12. Mozgovoi M.V. *C++ master-klass. 85 netrivial'nykh proektov, reshenii i zadach* (C++ Masterclass: 85 Nontrivial Projects, Solutions and Problems) (St. Petersburg: Nauka i Tekhnika, 2007).
13. Segaran T. *Programming Collective Intelligence* (Boston: O'Reilly Media, 2008; St. Petersburg: Simvol-Plyus, 2008).
14. Goldberger A.L., Amaral LAN, Glass L., Hausdorff J.M., Ivanov P.Ch., Mark R.G., Mietus J.E., Moody G.B., Peng C.-K., Stanley H.E. *Circulation*, **101**, e215 (2000); http://circ.ahajournals.org/content/101/23/e215.full.
15. Bousseljot R., Kreiseler D., Schnabel A. *Biomed. Tech.*, **40**, 317 (1995).